Journal of Hazardous Materials 166 (2009) 1272–1278

Contents lists available at ScienceDirect

Journal of Hazardous Materials

journal homepage: www.elsevier.com/locate/jhazmat

Kinetics and thermodynamics of textile dye adsorption from aqueous solutions using babassu coconut mesocarp

Adriana P. Vieira[a], Sirlane A.A. Santana[a], Cícero W.B. Bezerra[a], Hildo A.S. Silva[a], José A.P. Chaves[b], Júlio C.P. de Melo[c], Edson C. da Silva Filho[d], Claudio Airoldi[c,*]

[a] Departamento de Química/CCET, Universidade Federal do Maranhão, Av. dos, Portugueses S/N, Campus do Bacanga, 65080-540 São Luís, Maranhão, Brazil
[b] Colégio Universitário, Universidade Federal do Maranhão, 65080-540 São Luís, Maranhão, Brazil
[c] Institute of Chemistry, University of Campinas, UNICAMP, P.O. Box 6154, 13084-971 Campinas, São Paulo, Brazil
[d] Química, Universidade Federal do Piauí, 64900-000 Bom Jesus, Piauí, Brazil

ARTICLE INFO

Article history:
Received 4 September 2008
Received in revised form 8 December 2008
Accepted 8 December 2008
Available online 11 December 2008

Keywords:
Mesocarp
Babassu coconut
Adsorption
Dye textile

ABSTRACT

Extracted babassu coconut (*Orbignya speciosa*) mesocarp (BCM) was applied as a biosorbent for aqueous Blue Remazol R160 (BR 160), Rubi S2G (R S2G), Red Remazol 5R (RR 5), Violet Remazol 5R (VR 5) and Indanthrene Olive Green (IOG) dye solutions. The natural sorbent was processed batchwise while varying several system parameters such as stirring time, pH and temperature. The interactions were assayed with respect to both pseudo-first-order and second-order reaction kinetics, with the latter the more suitable kinetic model. The maximum adsorption was obtained at pH 1.0 for all dyes due to available anionic groups attached to the structures, which can be justified by pH_{pzc} 6.7 for the biosorbent BCM. The ability of babassu coconut mesocarp to adsorb dyes gave the order R S2G > VR 5 > BR 160 > IOG > RR 5, which data were best fit to Freundlich model, but did not well-adjusted for all dyes. The dye/biopolymer interactions at the solid/liquid interface are all spontaneous as given by free Gibbs energy, with exothermic enthalpic values of −26.1, −15.8, −17.8, −15.8 and −23.7 kJ mol^{-1} for BR 160, R S2G, RR 5, IOG and VR 5, respectively. In spite of the negative entropic values contribution, the set of thermodynamic data is favorable for all dyes removal. However, the results pointed to the effectiveness of the mesocarp of babassu coconut as a biosorbent for removing textile dyes from aqueous solutions.

1. Introduction

Water pollution is one of the most undesirable environmental problems in the world and it requires solutions. Textile industries produce a lot of wastewater, which contains a number of contaminants, including acidic or caustic dissolved solids, toxic compounds, and any different dyes. Many of the organic dyes are hazardous and may affect aquatic life causing various diseases and disorders [1]. Due to their chemical structures, dyes are resistant to fading on exposure to light, water and many chemicals and, therefore, are difficult to be decolorized once released into the aquatic environment [2].

Various techniques have been employed for dye removal from wastewaters. Currently, the principal methods of treatment involve biological, physical and/or chemical processes such as microbial degradation [3] chemical oxidation [4], electrofloculation [5] and adsorption [6]. However, these processes usually require appropriate facilities with high maintenance costs. Considering these diverse processes, adsorption has proven to be an effective procedure for removal of various pollutants from aqueous solutions and is also one of the most economical alternative technologies for the treatment of dye-contaminated waste streams. Up to now, activated carbon adsorption is commonly accepted to be the best available technology for dye reduction, although its manufacturing costs are in fact rather high. As is known, activated carbons are made from different plants, animal residues or bituminous coal [7]. Thus, it is desirable to search worldwide for a low cost source of an alternative adsorbent.

Some natural biomaterials including agricultural products and other by-products with low costs have been explored as new sources in recent years. Thus, dye removal by agricultural by-products and other low cost sorbents has also been intensively investigated. Materials deriving from agricultural by-products can be useful to convert unwanted, surplus agricultural waste, of which billions of kilograms are produced annually, into a useful adsorbent, a value-added advantage. Many specific examples are found where disposal of agricultural by-products has become a major, costly waste disposal problem [8].

Previous investigation on babassu coconut mesocarp (BCM) has demonstrated its ability for adsorbing a particular textile dye. Based

* Corresponding author. Tel.: +55 19 35213055; fax: +55 19 35213023.
E-mail address: airoldi@iqm.unicamp.br (C. Airoldi).

0304-3894/$ – see front matter © 2009 Elsevier B.V. All rights reserved.
doi:10.1016/j.jhazmat.2008.12.043

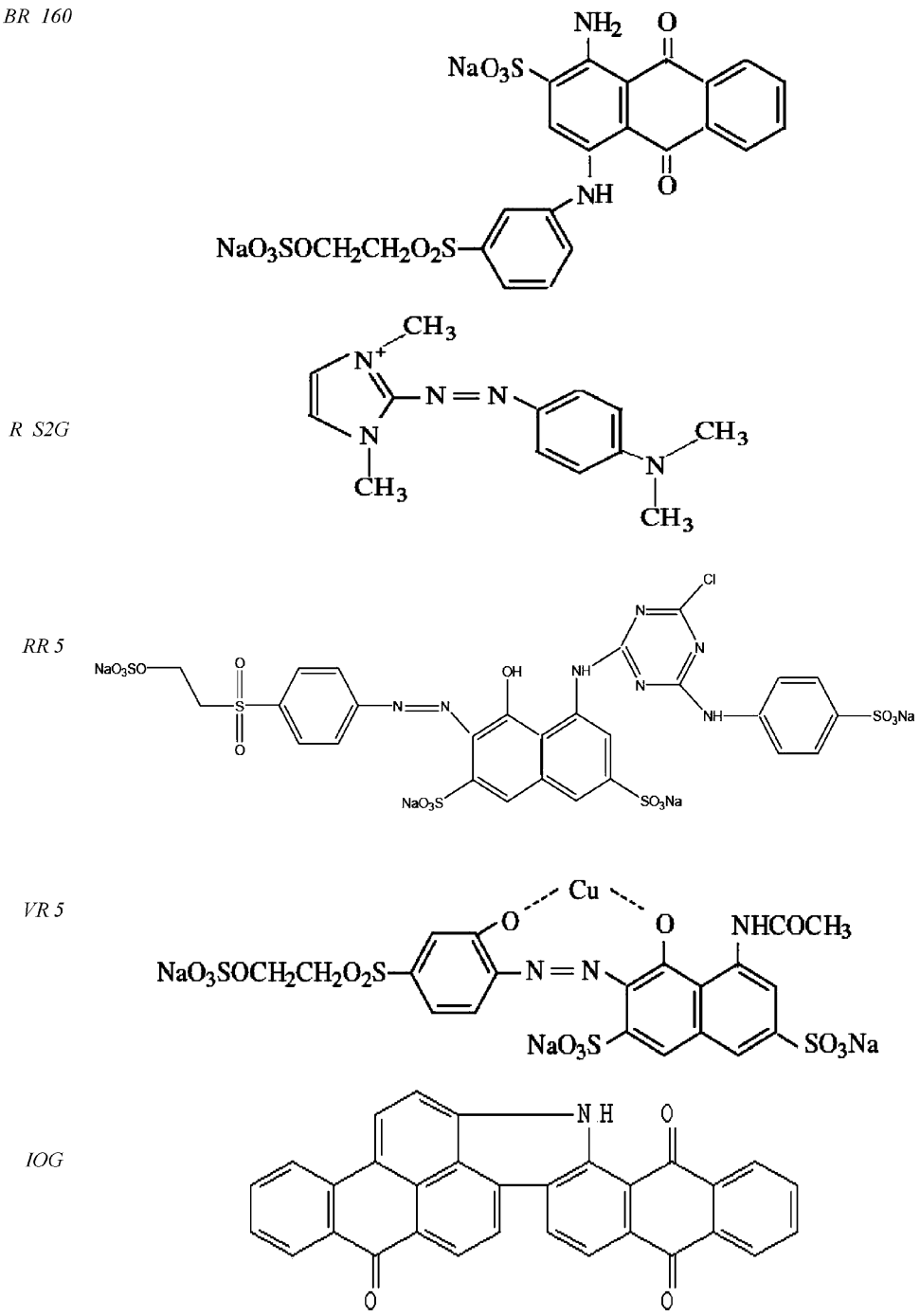

Fig. 1. Chemical structures of the dyes.

on this property, the present study will report some results involving water-soluble dyes found in wastewaters. The thermodynamics of this process is also reported.

2. Experimental

2.1. Materials and methods

The Blue Remazol 160 (BR 160), Ruby S2G (R S2G), Red Remazol 5 R (RR 5), Brilliant Violet Remazol 5R (VR 5) and Indanthrene Olive Green (IOG) dyes were provided by Indústria de Toalhas de São Carlos, state of São Paulo, Brazil. The respective chemical structures are shown in Fig. 1. All the dyes were chemical products of analytical grade and were used without further purification.

The babassu coconut mesocarp was acquired at a local market in São Luis, Maranhão, Brazil and was used after crushing the raw material into particle sizes in the 0.088–0.177 mm range. The infrared spectrum of the BCM sample was recorded on a Bomem FTIR, model MB Series, using KBr pellets, in the 4000–400 cm^{-1} wavelength range. Spectroscopy in the visible region was obtained in a quartz cell with path length of 1.0 mm. The spectra were recorded on a Cary 50 Varian spectrophotometer apparatus. The maximum wavelengths λ_{max} (nm) were determined to be 625, 470,

515, 560 and 620 nm, for BR 160, R S2G, RR 5, VR 5R and IOG, respectively.

2.2. Adsorption

For the kinetics studies 100 mg of adsorbent were mixed with 10.0 cm^3 aqueous dye solutions of known concentration at 298 ± 1 K, to give a dosage of 10.0 g dm^{-3}. The natural pH of these solutions was around 6.0, which did not change much with dilution. The series of flasks with solutions were then shaken and the changes of absorbance of all samples were monitored and determined after 5, 10, 20, 30, 60, 120 and 180 min during the adsorption process. After each adsorption was over, the mixture was rapidly filtered and the dye concentration determined. Equilibria were clearly established after 20 min for IOG and 30 min for the other dyes. The adsorption isotherm for each dye was studied through the batch method in which concentrations varied from 20 to 70 mg dm^{-3}, as a function of the time, established above, to reach the equilibrium condition. The amount adsorbed was estimated by the difference between the initial concentration in aqueous solution and that found in the supernatant. The amount of dye-adsorbed q_e (mg g^{-1}) was determined by:

$$q_e = \frac{C_i - C_f}{W} \times V, \quad (1)$$

where C_i and C_f are the initial and final dye concentrations at equilibrium in the aqueous phase (mg dm^{-3}), respectively, V is volume of dye solution (dm^3) and W is the mass of mesocarp employed.

2.3. pH influence

The pH dependency of the dye adsorption by BCM was carried out over the 1–12 range, by using DM-21 DIGMED and buffer solutions: pH 1 and 2 (KCl/HCl); pH 3 and 4 ($KHC_8H_4O_4$/HCl); pH 5 and 6 ($KHC_8H_4O_4$/NaOH); pH 8 and 9 (Borax/HCl); pH 10 and 11 (Borax/NaOH); pH 12 (KCl/NaOH). Samples of 100 mg of mesocarp were suspended with stirring with 10.0 cm^3 solutions of each dye, having known concentrations, and maintained under stirring for 1 h. Then, the mixture was filtered and the dye concentrations were determined by visible spectrophotometry.

2.4. Point of zero charge

The point of zero charge of babassu mesocarp coconut was determined by the solid addition method [9]. To a series of 100 cm^3 of conical flasks were transferred 20.0 cm^3 of solution with pH varying of 1–12 and the pH_0 values of each solution was adjusted by adding either 0.10 mol dm^{-3} of hydrochloric acid or sodium hydroxide. The pH_0 of the solutions were then accurately measured and 0.10 g of BMC was added to each flask, which was securely capped immediately. The suspensions were then manually shaken, allowed to equilibrate for 24 h with intermittent manual shaking and the pH values of the supernatant were measured. The difference between the initial and final pH value, $\Delta pH = pH_0 - pH_f$, was plotted against pH_0 and the point of intersection of the resulting null ΔpH corresponds to the point zero charge, pH_{PZC}.

3. Results and discussion

3.1. Infrared spectroscopy

The infrared spectrum for mesocarp as shown in Fig. 2 presents a large number of functional groups, that constitute this biomaterial, notably –OH in the 3400–3300 cm^{-1} interval, $-CH_2$ and CH_3 in the 2800–3000 cm^{-1} range, water at 1640 cm^{-1} and C–O–C between 1200–1000 cm^{-1}. The bands at 860, 769 and 710 cm^{-1} can be assigned to ester vibrations and monosubstituted aromatic rings, due to the lignin fraction in the raw material [10].

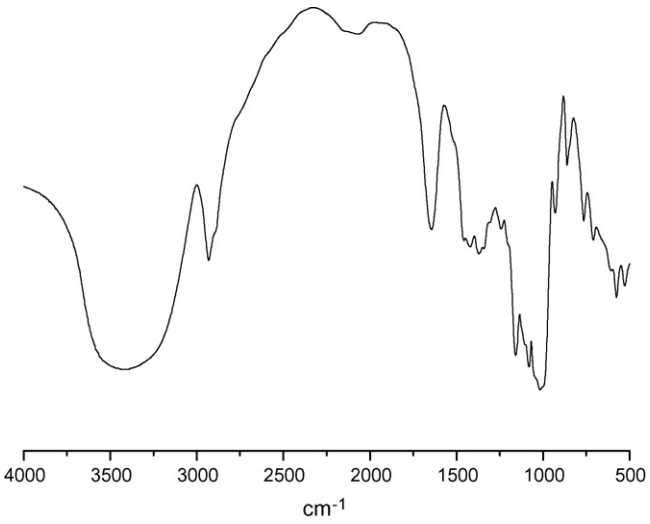

Fig. 2. FTIR of babassu coconut mesocarp.

3.2. Kinetics of adsorption

The kinetic results of the mesocarp adsorption process are shown in Fig. 3. These plots showed that the equilibrium was attained within a few minutes, by establishing a well-formed plateau, indicating also that the mesocarp was a very effective adsorbent for this short time for all textile dyes used. This adsorption contrasts with methylene blue on Neem leaf powder [11] and acid yellow and acid blue by activated carbon derived from rice husk [12], which used the same dosage of 10.0 g dm^{-3}, while the time to attain equilibrium was 1 and 10 h, respectively.

Based on the results obtained, the order of the adsorption is given by: R S2G > VR 5 > BR 160 > IOG > RR 5. The relative amount adsorbed is directly dependent on the respective structure of each dye, which can be chemically adjusted to the adsorbent surfaces in different forms.

To investigate the possible mechanism of adsorption, pseudo-first-order and pseudo-second-order adsorption models were fit to test the experimental data. The first order rate expression of

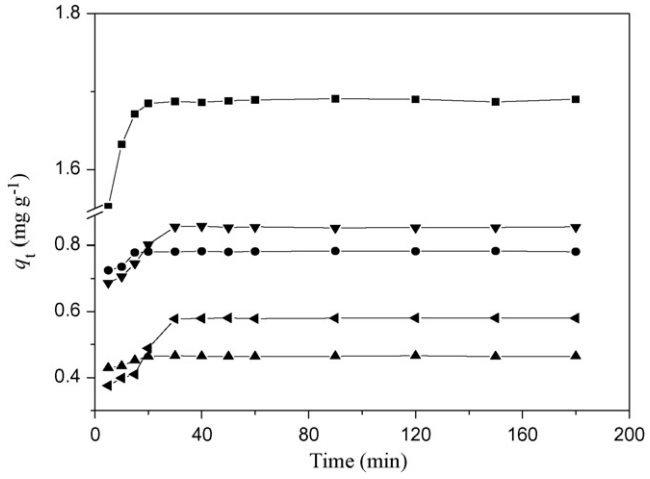

Fig. 3. Kinetics for Rubi S2G (R S2G) (■), Violet Remazol 5R (VR 5) (▼), Blue Remazol 160 (BR 160) (●) Indanthrene Olive Green (IOG) (◄) and Red Remazol 5R (RR 5) (▲) adsorptions by BCM at 298 ± 1 K and pH 6.

Lagergren [13] is given as:

$$\frac{dq_t}{dt} = k_1(q_e - q_t) \quad (2)$$

where q_e and q_t are the amounts of dye adsorbed on adsorbent (mg g^{-1}) at equilibrium and at time t, respectively, and k_1 is the rate constant of this adsorption (min^{-1}). Integrating Eq. (2), after applying the initial condition of $q_t = 0$ at $t = 0$ gives the linear form in Eq. (3):

$$\log(q_e - q_t) = \log q_e - \frac{k_1 t}{(2.303)}, \quad (3)$$

From this equation the slopes and intercepts of $\log(q_e - q_t) \times t$ plots were used to determine the constant k_1.

For the second kinetic model [14] the expression is given by:

$$\frac{dq_t}{dt} = k_2(q_e - q_t)^2, \quad (4)$$

where k_2 (g mg^{-1} min^{-1}) is the rate constant of second-order adsorption. Similarly, the following equation can be obtained after integration to give the linear form:

$$\frac{t}{q_t} = \frac{1}{k_2 q_e^2} + \frac{t}{q_e} \quad (5)$$

The slopes and intercepts of t/q_t versus t plots were used to calculate the second-order rate constant k_2 and q_e. Here, the initial adsorption rate, h, is:

$$h = k_2 q_e^2, \quad (6)$$

The $\log(q_e - q_t) \times t$ plot indicates the invalidity of Lagergren equation for the present system and also explains that the process does not follow pseudo-first-order kinetics. A better linearity was obtained for pseudo-second-order kinetic plots, as shown in Fig. 4. Also, as shown in Table 1, the values of q_e from the pseudo-second-order kinetics are in agreement with experimental data, $q_{e,exp}$, with R^2 values in the range of 0.950–0.999. Similar second-order kinetics was found for adsorption of the dyes BR22 and AR114 on biosorbent waste product pith [15]. This tendency also has been reported for adsorption of dyes on various other non-conventional adsorbents [16]. Due to the different nature of the adsorbent used in the present investigation from those described above, a direct comparison of the k_2 values is not possible.

3.3. Adsorption isotherms

Profiles of the adsorption isotherms of IOG, R S2G, VR 5, BR 160 and RR 5 from aqueous solutions onto BCM are shown in Fig. 5. The Freundlich model [17] was used to describe the adsorption isotherm by the equation:

$$q_e = K_f C_e^{1/n} \quad (7)$$

where q_e is the amount of dye adsorbed at equilibrium in unit mass of BCM, C_e is the concentration of the dye in the aqueous phase at equilibrium, and n and K_f are Freundlich coefficient constants of the system. These values are good indicators of adsorption capacity and adsorption intensity, respectively. Eq. (7) may be linearized by taking the logarithmic form:

$$\log q_e = \log K_f + \frac{1}{n} \log C_e \quad (8)$$

The linear Freundlich plots, as shown in Fig. 6, were obtained by plotting $\log q_e$ versus $\log C_e$ and the adsorption coefficients were obtained from the slopes and the intercepts of the straight line. The adsorption coefficients determined from these plots are listed in Table 2. The Freundlich isotherm model is proposed for

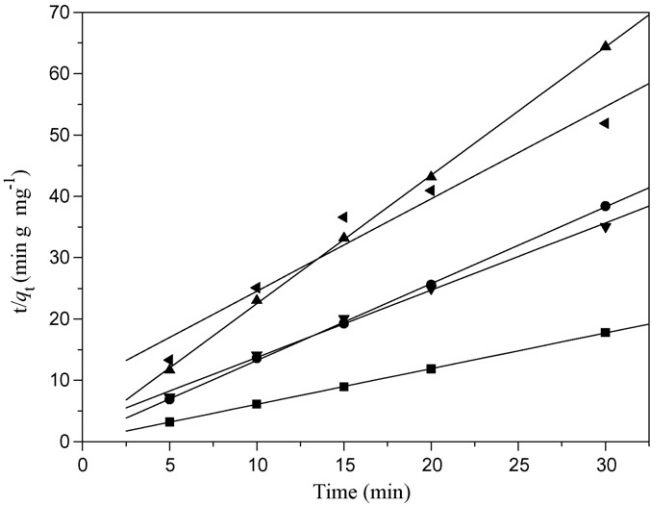

Fig. 4. Pseudo second-order plots for Red Remazol 5R (RR 5) (▲), Indanthrene Olive Green (IOG) (◀), Blue Remazol 160 (BR 160) (●), Violet Remazol 5R (VR 5) (▼) and Rubi S2G (R S2G) (■) adsorptions by BCM.

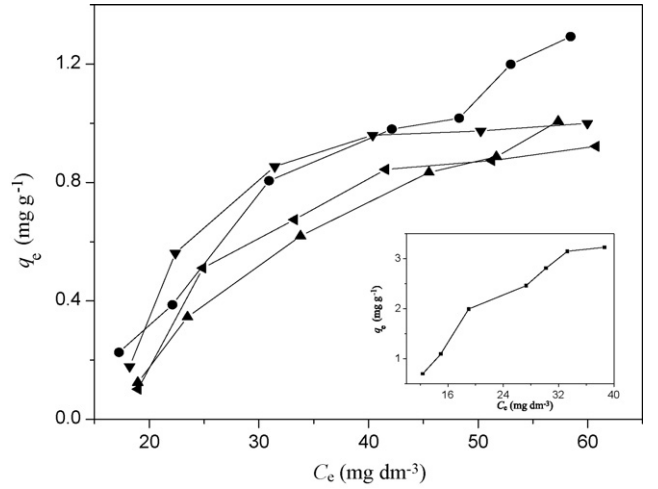

Fig. 5. Isotherms of Blue Remazol 160 (BR 160) (●), Violet Remazol 5R (VR 5) (▼), Indanthrene Olive Green (IOG) (◀), Red Remazol 5R (RR 5) (▲) and Rubi S2G (R S2G) (■) adsorptions by BCM at 298 ± 1 K and pH 6.

Table 1
Kinetic parameters for the removal of BR 160, R S2G, RR 5, IOG and VR 5 by BCM. Initial dye concentration of 40.0 mg dm^{-3} with dosage of 10.0 g of mesocarp per liter at pH 6.0 and 298 ± 1 K.

Dyes	$q_{e,exp}$ (mg g^{-1})	Pseudo-first-order			Pseudo-second-order			
		$q_{e,cal}$ (mg g^{-1})	k_1 (min^{-1})	R^2	$q_{e,cal}$ (mg g^{-1})	k_2 (g mg^{-1} min^{-1})	h (mg g^{-1} min^{-1})	R^2
BR 160	0.783	0.106	0.153	0.790	0.799	2.149	1.369	0.999
R S2G	1.690	0.248	0.160	0.936	1.719	1.180	3.487	0.999
RR 5	0.466	0.131	0.177	0.864	0.477	2.768	0.630	0.999
IOG	0.580	0.935	0.171	0.789	0.664	0.238	0.105	0.950
VR 5	0.857	0.0.931	0.149	0.420	0.911	0.4337	0.360	0.994

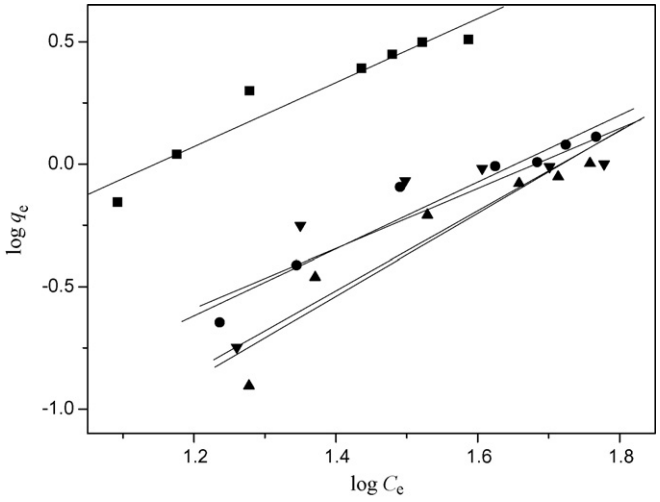

Fig. 6. Plots for Freundlich adsorption isotherms for Rubi S2G (R S2G) (■), Blue Remazol 160 (BR 160) (●), Red Remazol 5R (RR 5) (▲), Violet Remazol 5R (VR 5) (▼) and Indanthrene Olive Green (IOG) (◄) adsorptions by BCM at 298 ± 1 K and pH 6.

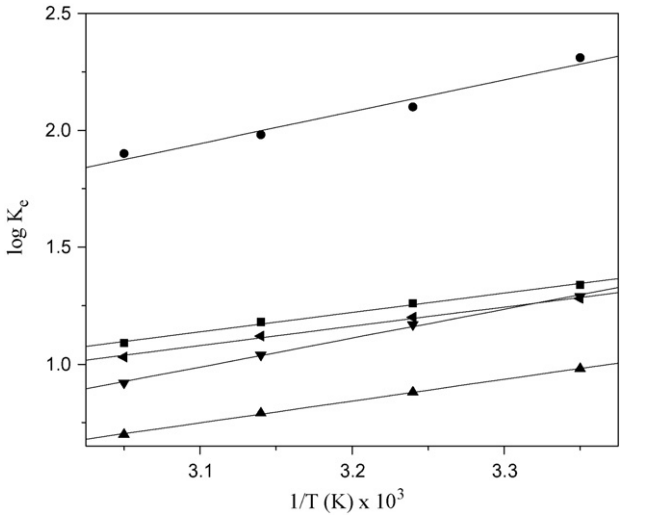

Fig. 7. van't Hoff plots for Blue Remazol 160 (BR 160) (●), Rubi S2G (R S2G) (■), Indanthrene Olive Green (IOG) (◄),Violet Remazol 5R (VR 5) (▼) and Red Remazol 5R (RR 5) (▲) adsorptions by BCM.

reversible adsorption and it is not restricted to the formation of a monolayer. The equation predicts that the dye concentration on the adsorbent is directly dependent on its quantity in liquid solution and the amount adsorbed is the summation of adsorption on all sites. Although the obtained data were better adjusted to this model, however, the fit for IOG and VR 5 dyes were not completely observed.

3.4. Thermodynamic processes

The set of thermodynamic parameters for the adsorption process, such as the Gibbs free energy (ΔG°), enthalpy (ΔH°) and entropy (ΔS°) of adsorption were determined by carrying out the adsorption experiments at four different temperatures [18], using the following equations:

$$\Delta G^\circ = \Delta H^\circ - T\Delta S^\circ \quad (9)$$

$$\log \frac{q_e}{C_e} = \frac{-\Delta H^\circ}{2.303RT} + \frac{\Delta S^\circ}{2.303R} \quad (10)$$

where (q_e/C_e), which correspond to the K_e values, is called the adsorption affinity and corresponds to the ratio of q_e, related to the amount adsorbed per unit mass (mg g^{-1}), and C_e, the equilibrium concentration (mg dm^{-3}) of the solute. The values of ΔH° and ΔS° were determined from the slope and the intercept of the linear plot of log K_e versus $1/T$ and from these values ΔG° was calculated.

The effect of temperature on adsorption was studied at 298, 308, 318 and 328 ± 1 K, by considering a suspended mesocarp amount of 100 mg in 10 cm^3, which was constantly stirred for 1 h. The amount of dye adsorbed on the mesocarp per unit mass gave a linear decrease with the increase in temperature. The van't Hoff plots of log K_e versus $1/T$ are shown in Fig. 7. The values obtained for the thermodynamic parameters from these plots are given in Table 3.

Table 2
Freundlich coefficients for BR 160, R S2G, RR 5, IOG and VR 5 adsorption on BCM at 298 ± 1 K.

Dye	R^2	n	K_f (dm^3 g^{-1})
BR 160	0.94	0.73	0.0055
R S2G	0.92	0.76	0.0317
RR 5	0.90	0.59	0.0012
IOG	0.85	0.61	0.0016
VR 5	0.84	0.82	0.0088

The exothermic enthalpy for the dye adsorption process gave values in the −26.1 to −15.8 kJ mol^{-1} range, indicating that chemisorptive bond formation between the dye molecules and the adsorbent surface is not strong in nature, as listed in Table 3. However, the spontaneity of wastewater dye adsorption on mesocarp is represented by the negative Gibbs free energy, even though all negative entropic values are unfavorable, which reflect an ordering arrangement of the water molecules initially bonded to the biopolymer or to the dye as the chemisorption progresses [19,20]. Taking into account the complete thermodynamic data on the dye/mesocarp interaction equilibrium, these values suggest that this kind of material could be explored for practical applications. Similar sets of thermodynamic data were previously obtained from chitosan-Reactive red dye wastewater under acidic or basic conditions [21].

3.5. pH effect

The pH of the solution affects the surface charge of the adsorbents as well as the degree of ionization and speciation of different pollutants. Change in pH affects the adsorptive process through dissociation of functional groups of the active sites on the surface of the adsorbent [22]. In this present case, when the experiments were carried out between pH 1.0–12.0, it was observed that dye adsorption presented the highest value at pH 1.0, after which the adsorption decreased continuously. For example, while at pH 6.0 the maximum quantity of dye removal was 43.4% for R S2G, at pH 1.0, the quantity removed was higher than 90% for all dyes, reaching 99.5% for BR 160, as shown in Fig. 8.

The effect of pH on dye adsorption can be interpreted on the basis of surface hydroxylation, acid–base dissociation and surface complex formation [23–25]. It is suggested that the increase in sorption at lower pH depends not only on the properties associated with the adsorbent surface, but also the dye structure, as under these conditions a higher uptake of anionic dyes occurred in an acidic medium, compared to a basic medium [26]. This is in agreement with the results obtained in the present investigation with the series of dye solutions, in which it is expected that the mesocarp surface had more preference for the dissociated anionic species of the dyes near pH 1.0.

From the structural point of view BCM contains a large number of functional groups, phenolic as well as carboxylated groups. The interaction of the dye molecules with these functional groups

Table 3
Thermodynamic data for BR 160, R S2G, RR 5, IOG and VR 5 adsorption on BCM for dye concentrations of 40.0 mg dm^{-3} with dosage of 10.0 g of mesocarp per liter, agitation time 60 min and pH 6.0.

Dye	$-\Delta H^{\circ}$ (kJ mol^{-1})	$-\Delta S^{\circ}$ (J mol^{-1} K^{-1})	$-\Delta G^{\circ}$ (kJ mol^{-1})				R^2
			298 K	308 K	318 K	328 K	
BR 160	26.1	44	13.2	12.4	12.1	11.9	0.970
R S2G	15.8	27	7.6	7.4	7.2	6.8	0.994
RR 5	17.8	41	5.6	5.2	4.8	4.4	0.998
IOG	15.8	28	7.3	7.1	6.8	6.5	0.994
VR 5	23.7	55	7.4	6.9	6.3	5.9	0.998

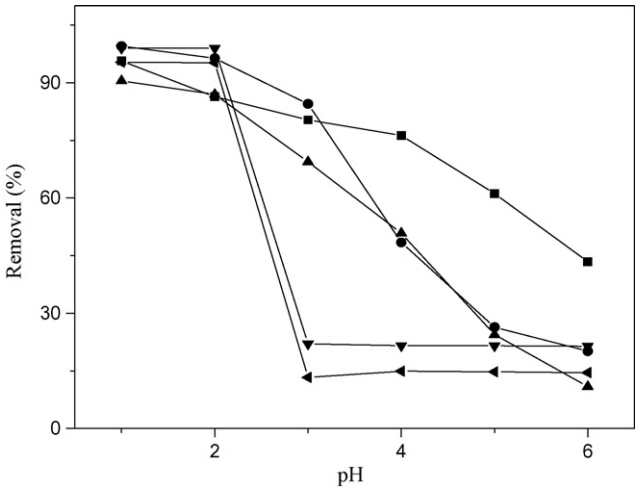

Fig. 8. Effect of pH on adsorptions of Blue Remazol 160 (BR 160) (●), Rubi S2G (R S2G) (■), Red Remazol 5R (RR 5) (▲), Violet Remazol 5R (VR 5) (▼) and Indanthrene Olive Green (IOG) (◄) dyes by BCM. Adsorbent dose, 10 g dm^{-3}; agitation time, 60 min; $T = 298 \pm 1$ K.

may follow an extremely complicated pattern. However, the effect of pH at the solid–liquid equilibrium can be explained on the basis of chemical interactions: (i) between phenolic hydroxyl groups on the biosorbent with active centers on the dyes, (ii) other chemical interactions between carboxylate groups with the cationic dye fraction and, (iii) finally, weak electrostatic interactions between the cationic dye and electron-rich sites of mesocarp surface, such was previously suggested for other biosorbents [11].

The success of the adsorption process is closely dependent on the presence of available counter-ions to retain the desirable species on the surface. For example, at lower pH the attached proton can easily adsorb anions, while an inverse behavior occurs at high pH due to the hydroxyl groups at the solid/liquid interface [12]. The understanding of the adsorption mechanism can be elucidated through the point of zero charge (pH_{PZC}) of the adsorbent determination. Thus, the adsorption of cations is favored at $pH > pH_{PZC}$, while the opposite is observed for anions. For the present adsorbent the zero value of ΔpH lies at the initial pH value of 6.7, as shown in Fig. 9. It is noticed that the surface of the adsorbent changes its polarization according to the pH value of the solution and to the point of zero charge of the solid. As observed, at pH values lower than pH_{PZC} the surface becomes positively charged, then it is expected the adsorption of these dyes are favorable, due to the presence of several functional groups such as OH^-, COO^- or SO_3^{2-} groups.

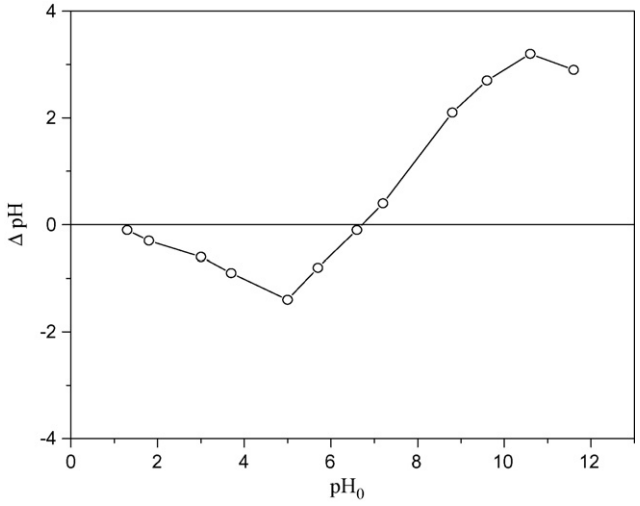

Fig. 9. Point of zero charge of BCM.

4. Conclusion

This study demonstrated that BCM biopolymer is an effective adsorbent for textile dye removal from aqueous solutions, by assaying 10.0 g of the adsorbent per liter of aqueous solution. The resulting solution is decolorized by as much as 43.4% for R S2G in aqueous solution, after stirring the suspension for 1 h, at pH 6.0, which is the natural pH of the dye solution. A decrease in pH strongly affects the adsorption process, reaching a maximum value of 99.5% for BR 160 at pH 1.0, that is justified by the point of zero charge (pH_{PZC}). The adsorption data was adjusted to Freundlich isotherms and the kinetic data follows second-order kinetic models. The set of thermodynamic data for all dyes on BCM gave exothermic enthalpic values, with the dye removal capacity decreased as the temperature increased, probably due to increasing mobility of the dye molecules during the adsorption process. In spite of the negative entropic values, the contribution of the exothermic enthalpy gave results that reflected the spontaneity of adsorption process, which suggests the use of this biopolymer for dye removal from industrial wastewaters. Finally, this biopolymer, unexplored so far for this use, seems to be an excellent alternative, as it is an abundant biomass available at low cost.

Acknowledgements

The authors are indebted to CAPES for financial support, to the Indústria de Toalhas São Carlos for donation of the dye samples, to FAPEMA for a fellowship to APV and to CNPq for a fellowship to CA.

References

[1] G. McKay, G.A. Sweeney, Principles of dye removal from textile effluent, Water Air Soil Pollut. 4 (1980) 3–11.
[2] G. McKay, Waste color removal from textile effluents, Am. Dyest. Rep. 68 (1979) 29–36.
[3] N.D. Lourenço, J.M. Novais, H. Pinheiro, Kinetic studies of reactive azo dye decolorization in anaerobic/aerobic sequencing batch reactors, Biotechnol. Lett. 28 (2006) 733–739.
[4] L. Núnez, J.A.G. Hortal, F. Torrades, Study of kinetic parameters related to the decolorization and mineralization of reactive dyes from textile dyeing using Fenton and photo-Fenton processes, Dyes Pigm. 75 (2007) 647–652.

[5] C.L. Yang, J. McGarrahan, Electrochemical coagulation for textile effluent decolorization, J. Hazard. Mater. B127 (2005) 40–47.
[6] D.W. O'Connell, C. Birkinshaw, T.F. O'Dwyer, Heavy metal adsorbents prepared from the modification of cellulose: a review, Bioresour. Technol. 99 (2008) 6709–6724.
[7] A.R. Dinçer, Y. Günes, N. Karakaya, E. Günes, Comparison of activated carbon and bottom ash for removal of reactive dye from aqueous solution, Bioresour. Technol. 98 (2007) 834–839.
[8] G. Crini, Non-conventional low-cost adsorbents for dye removal: a review, Bioresour. Technol. 97 (2006) 1061–1085.
[9] L.S. Balistrieri, J.W. Murray, The surface chemistry of goethite (α-FeOOH) in major ion seawater, Am. J. Sci. 281 (1981) 788–806.
[10] V. Tserki, P. Matzinos, S. Kokkou, C. Panayiotou, Novel biodegradable composites based on treated lignocellulosic waste flour as filler. Part I. Surface chemical modification and characterization of waste flour, Composites A 36 (2005) 965–974.
[11] K.G. Bhattacharyya, A. Sharma, Kinetics and thermodynamics of methylene blue adsorption on neem (*Azadirachta indica*) leaf powder, Dyes Pigm. 65 (2005) 51–59.
[12] M.M. Mohamed, Acid dye removal: comparison of surfactant-modified mesoporous FSM-16 with activated carbon derived from rice husk, J. Colloid Interface Sci. 272 (2004) 28–34.
[13] S.J. Allen, Q. Gan, R. Matthews, P.A. Johnson, Kinetic modeling of the adsorption of basic dyes by kudzu, J. Colloid Interface Sci. 286 (2005) 101–109.
[14] Y.S. Ho, G. McKay, Pseudo-second order model for sorption processes, Process Biochem. 34 (1999) 451–465.
[15] Y.S. Ho, G. McKay, Sorption of dye from aqueous solution by peat, Chem. Eng. J. 70 (1998) 115–124.
[16] Y.S. Ho, Review of second-order models for adsorption systems, J. Hazard. Mater. B136 (2006) 681–689.
[17] Y.C. Wong, Y.S. Szeto, W.H. Cheung, G. McKay, Effect of temperature, particle size and percentage deacetylation on the adsorption of acid dyes on chitosan, Adsorption 14 (2008) 11–20.
[18] Y. Önal, Kinetics of adsorption of dyes from aqueous solution using activated carbon prepared from waste apricot, J. Hazard. Mater. B137 (2006) 1719–1728.
[19] M.O. Machado, A.M. Lazarin, C. Airoldi, Thermodynamic features associated with intercalation of some *n*-alkylmonoamines into barium phosphate, J. Chem. Thermodyn. 38 (2006) 130–135.
[20] D.L. Guerra, C. Airoldi, K.S. Sousa, Adsorption and thermodynamic studies of Cu(II) and Zn(II) on organofunctionalized-kaolinite, Appl. Surf. Sci. 254 (2008) 5157–5163.
[21] N. Sakkayawong, P. Thiravetyan, W. Nakbanpote, Adsorption mechanism of synthetic reactive dye wastewater by chitosan, J. Colloid Interface Sci. 286 (2005) 36–42.
[22] H.A. Elliott, C.P. Huang, Adsorption characteristics of some Cu(II) complexes on alumino silicates, Water Res. 15 (1981) 849–854.
[23] B.C. Raymahashay, A comparative study of clay minerals for pollution control, J. Geol. Soc. India 30 (1987) 408–413.
[24] M.S. El-Geundi, Color removal from textile effluents by adsorption techniques, Water Res. 25 (1981) 271–279.
[25] C.K. Lee, K.S. Low, S.W. Chow, Chrome sludge as an adsorbent for color removal, Environ. Technol. 17 (1996) 1023–1028.
[26] M.-S. Chiou, P.-Y. Ho, H.-Y. Li, Adsorption of anionic dyes in acid solutions using chemically cross-linked chitosan beads, Dyes Pigm. 60 (2004) 69–84.